# A Two-Fidelity Level Approach for Marine Propeller Design

**Stefano Gaggero**[1,*], **Giuliano Vernengo**[1], **Diego Villa**[1]

[1] Department of Naval Architecture, Electric, Electronic and Telecommunication Engineering, University of Genoa, Via Montallegro 1, 16145, Genoa, Italy

[*] Corresponding author: Stefano Gaggero, stefano.gaggero@unige.it

## ABSTRACT

A Simulation Based Design Optimization method for marine propellers using a two-fidelity levels meta-model for global design space exploration and optimization is presented. Response surfaces are built using the co-Kriging approximation, i.e. a multi-output Gaussian process that combines large low-fidelity dataset with few, costly, high-fidelity data. The method is applied for the CFD-based shape optimization of the E779A propeller using, as fidelity levels, two different physical models for the propeller performances prediction, namely a Boundary Element Method (low-fidelity) and a RANSE solver (high-fidelity). Results demonstrate the feasibility of multi-objective, constrained, design procedures, like those involving marine propellers, using these multi-fidelity response surfaces. At the same time, the need of good correlations between low- and high- fidelity data feeding the surrogate models is highlighted as a requisite for robust and reliable predictions using these approximated methods.

**Keywords**: Propeller Design; Gaussian Process; Optimization; Multi-fidelity;

## 1 INTRODUCTION

The fluid-dynamic design of complex engineering systems is a process that involve experience, physical insight and computational tools. These steps are more and more often supplemented by a formal optimization strategy that permits a wider exploration and a fine-tuning of the design. Automatic Simulation Based Design Optimization (SBDO) formulations of the design problem have become a useful support to the decision-making process and could help designers to make sound decisions, especially for innovative configurations, by providing rational and organized quantifications of the Key Performance Indicators (KPI) of the system under investigation. One of the crucial issue in SBDO approaches, unfortunately, is the trade-off between the accuracy of design data and the computational effort that is required to gather those data. SBDO are usually implemented as an iterative process, combining design modification methods, numerical simulations and optimization algorithms to identify new, optimized, designs. They basically rely on a "try-and-error" procedure which has to deal with two conflicting task if a reliable and usable SBDO is needed. On one side the objective functions evaluation must rely on high-fidelity, physics-based solvers to accurately capture the physics of the phenomena under investigation, allowing the exploration (not sustainable by fast computational tools) of wider design spaces, including for instance non-conventional configurations not accounted by traditional design approach and far from usual and well-established design guidelines. On the other side, the need to deal with larger design space requires a large number of such expensive evaluations to converge to the final solution especially in the case of the existence of local optima that forces the use of costly derivative free global optimization methods and makes the SBDO process hardly affordable when computational resources and time are limited.

Recently, the design of marine propellers underwent radical modifications as well, and now SBDO approaches represent a valid alternative to usual lifting line/lifting surface design methods, especially in the case of unconventional propulsors (Gaggero et al., 2016). To comply with the need of computationally efficient evaluations of the KPI of the design, and to explore thoroughly the design space in reasonable design times, however, mainly Boundary Element Methods were adopted as flow solver in

these iterative design processes. For sure BEM are a step forward compared to other potential flow formulations for what regards the possibility, for instance, to deal with cavitation or for what concern the rigorous description of the geometry (i.e. ducted propellers). But in some specific applications their inherited limitations could nullify the reliability of the results of the design process, making the effort of a SBDO useless. These are the few examples to which RANSE based SBDO have been reserved to (Gaggero, 2020) even if, due to computational effort required for such calculations, the number of free parameters, as well as their range of variation and the total number of iterations, was limited, leaving the feeling that larger gains would have been possible with a more extensive investigation.
In this context, metamodel methods have been developed and successfully applied. Metamodels provide an approximated representation of expensive simulations using only few of them: a sort of "trained black box" that can substitute the real calculations into the optimization activity. Kriging, Radial Basis Functions, Neural networks, among the others, are some of the approaches that were successfully used in the maritime field to built these approximations, leading to affordable SBDO for the optimization of the hull shape, of the propeller blades geometry or of several energy saving devices, considering simultaneously contrasting objectives and performance constraints (Serani et al., 2019; Coppedè et al., 2019; Raven and Sholcz, 2019). Adaptive sampling techniques of the design space, exploiting the information that becomes available during the analysis process, have been developed as well (Serani et al., 2019) to improve the fitting capabilities of the surrogate models by adding training points only where they are most useful and, then, by keeping to the lowest possible the number of expensive evaluations of the key performance indexes over which the metamodel is built.
Similarly, also multi-fidelity models have been developed with the aim of further reducing the computational cost of SBDO without sacrificing their accuracy and, consequently, the reliability of the design results. Multi-fidelity techniques combine the trends easily attainable by a large number of low-fidelity simulations with the accuracy of only few high-fidelity calculations that "correct" the results from the low-fidelity model, building (and dynamically updating, if required) more reliable surrogate models of the phenomena under investigation. Radial Basis Function and co-Kriging (Wang and Shan, 2007; de Baar et al., 2015) are the most used approaches that, in CFD-based analysis/optimization procedures, usually make use of different physical models like potential flow, RANSE solver or experimental measurements, (Gaggero et al., 2019) and numerical accuracies (i.e. grid size and simulation time step) to realize the necessary number of fidelity levels required to improve the prediction accuracy at the minimum additional cost of the final metamodel.
Propeller design can easily take advantage of these paradigms thanks to the availability of computational tools for propeller performance characterization that have been already applied, separately and with success, in SBDO processes. Low-fidelity BEM computations have already proven to be useful for the identification of improved propeller geometries, which final performances were obviously verified using RANSE calculations. The logical step of this design process is to include directly in the searching procedure of the optimal the results of high-fidelity analyses, such RANSE, rather than using them only in the post-processing phase. Multi-fidelity metamodels built using Bayesian inference techniques like the co-kriging model proposed in this work, permit the realization of these high-quality response surfaces. By replacing any direct evaluation of the key performance indexes in the optimization process they allow to explore more reliably and extensively (thanks to the inclusion of the "correction" provided by the high-fidelity analyses) and more quickly than any SBDO based on direct low-fidelity calculations, the enlarged design spaces often required for performance improvements.
In light of this, current paper proposes a Simulation Based Design Optimization process for the design of marine propellers based on a two-fidelity level co-Kriging approach (respectively BEM for low-fidelity and RANSE for high-fidelity analyses) for the approximations of the propeller key performance indexes (KPI) used in the optimization. A simple literature test case, the E779A propeller is considered to prove the effectiveness of the multi-fidelity metamodels, and to investigate the optimal balance between low- and high- fidelity data to realize robust and reliable response surfaces. To this aim the complexity of the design, especially for what concern the parametric description of the geometry, is lowered compared to real cases by considering only four design parameters, i.e. those that describe the blade pitch distribution. This permits a better handling and visualization of results,, which is of

utmost importance in this preliminary assessment of the merits of the proposed design framework.

# 2 NUMERICAL TOOLS

## 2.1 The co-Kriging surrogate model

Co-Kriging metamodels are a special case of multi-output Guassian Processes that exploit the correlation between different fidelity levels of data to enhance the predictive accuracy and make the best approximation of the high-fidelity data over the design space. A co-Kriging metamodel can be interpreted as a combination of two Kriging models (Forrester et al., 2007; Couckuyt et al., 2014) built sequentially. The first Kriging model $Y_{lf}(\mathbf{x})$ is constructed using the low-fidelity data $((X_{lf}, \mathbf{y}_{lf})$, being $X_{lf} = \{\mathbf{x}^1_{lf}, ..., \mathbf{x}^{n_{lf}}_{lf}\}$ the $n_{lf}$ sampling points and $\mathbf{y}_{lf} = \{\mathbf{y}^1_{lf}, ..., \mathbf{y}^{n_{lf}}_{lf}\}$ the associated values). The second Kriging model $Y_\Delta(\mathbf{x})$ is constructed, instead, on the residuals between the high-fidelity data and the low-fidelity predictions $(X_{hf}, \mathbf{y}_\Delta)$, where $\mathbf{y}_\Delta = \mathbf{y}_{hf} - \rho \cdot Y_{lf}(X_{hf})$. In this expression $Y_{lf}$ is the low-fidelity Kriging model evaluated in the available $n_{hf}$ high-fidelity samples $X_{hf} = \{\mathbf{x}^1_{hf}, ..., \mathbf{x}^{n_{hf}}_{hf}\}$ and $\mathbf{y}_{hf} = \{\mathbf{y}^1_{hf}, ..., \mathbf{y}^{n_{hf}}_{hf}\}$ the corresponding high-fidelity values. The idea beneath this approach is that the difference $\mathbf{y}_\Delta$ is a smaller quantity, with a simpler distribution to be approximated using the limited data set of high-fidelity data if the correspondence between low- and high-fidelity levels is sufficient. Similarly to a single-fidelity Kriging model, also the co-Kriging formulation exploits correlation matrices and process variances, in this case for both low-fidelity data and residuals, to realize the metamodel. The scaling factor $\rho$ is evaluated, simultaneously to the hyperparameters of the correlation functions (in this case the Matern $\nu = 3/2$), as a part of the Maximum Likelihood Estimation.

## 2.2 Boundary Element Method

Low-fidelity calculations were carried out using the Boundary Element Method developed at the University of Genoa (Gaggero et al., 2014). The method is based on the Morino formulation (Morino and Kuo, 1974) and it uses the *key-blade* to handle the unsteadiness when the propeller operates in the wake of a ship. Cavitation analyses include the prediction of steady and unsteady sheet bubbles on both suction and pressure side.

The reference surface mesh adopted for calculations is that of Figure 1. It consists of 1500 panels per blade and a trailing wake realized with an equivalent time step of 6 deg. Current calculations account only for steady, non-cavitating, pressure distributions (and performances), which were collected at the advance coefficient selected for the optimization ($J = 0.833$), in several zones of the blade. They reflect the need of considering the risk of different types of cavitation using the simplest cavitation inception criterion ($-C_{PN} > \sigma_N$) at the leading edge ($0 < x/x < 0.2$) and at midchord ($0.2 < x/c < 0.6$), at the tip ($r/R > 0.7$) and at the root ($r/R < 0.7$) of the blade, on both the suction and the pressure side. The minimum values of pressure over the eight patches that describe the critical zones of the blade, in this context, represent together with propeller efficiency and the delivered thrust, the key performance indexes of the design and, then, of the optimization.

Under these simplified assumptions, each computation runs in less than 20 seconds, making the BEM an excellent candidate for the analysis of the hundreds/thousands of configurations that sample the design space and provide data to feed the low-fidelity response surfaces of the design KPI.

## 2.3 RANS Calculations

RANS equations were used to provide the co-Kriging models with high-fidelity data. Calculations were carried out using StarCCM+ on a polyhedral mesh (that of Figure 1) of about 1 Million elements. Also in this case, since analyses are steady and non-cavitating, the periodicity of the propeller geometry was exploited by solving only one blade passage realized with appropriate periodic boundary conditions. Turbulence was addressed using the two-equations *realizabke* $k - \epsilon$ model. Together with 5 prism layers, it ensures an average non-dimensional wall distance of about 40. Accordingly with BEM

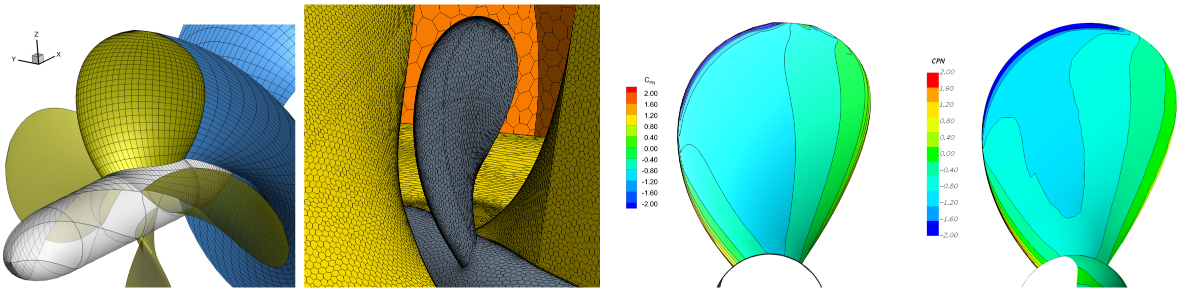

(a) Mesh, BEM (b) Mesh, RANS (c) $C_{PN}$, BEM (d) $C_{PN}$, RANS

**Figure 1**. Reference meshes arrangement and pressure distribution over the blade at the design advance coefficient. KPI by BEM : $K_T = 0.174$, $\eta_o = 0.680$, $C_{PN,LE,back,root} = -1.52$, $C_{PN,LE,back,tip} = -5.45$, $C_{PN,Midchord,back,root} = -1.02$, $C_{PN,Midchord,back,tip} = -0.99$, $C_{PN,LE,face,root} = -0.78$, $C_{PN,LE,face,tip} = -0.33$. KPI by RANS: $K_T = 0.173$, $\eta_o = 0.676$, $C_{PN,LE,back,root} = -1.59$, $C_{PN,LE,back,tip} = -7.10$, $C_{PN,Midchord,back,root} = -0.97$, $C_{PN,Midchord,back,tip} = -0.95$, $C_{PN,LE,face,root} = -0.63$, $C_{PN,LE,face,tip} = -1.89$.

analyses, the same KPIs collected by the low-fidelity model, namely the propeller performances and minimums of the pressure over the same eight patches of the blade, have been extracted from RANS calculations. Regardless the simplification accepted for the design (steady calculations, cavitation risk using the non-cavitating pressure coefficient only), the run time of each case, on a medium-end workstation, is of about one hour. As discussed, while this represents the most serious bottleneck for the realization of a completely RANS based SBDO, it instead can be easily afforded for the (very) sparse sampling of the design space that is sufficient to train reliable co-Kriging surrogate models.

## 2.4 Propeller blade variations

Compared to similar shape optimization problems (i.e. ship hulls) for which complex tools like free-form deformations or indirect parametrization of the geometry are needed (Coppedè et al., 2019; Coppedé et al., 2018), a robust parametric description of the propeller blade is naturally provided by its design table. Following well-established procedures (Gaggero et al., 2016), also in this case the parametrization is realized using B-Spline curves, which flexibility for this specific application is unrivaled by any other descriptions.

As discussed in the introduction, only the blade pitch distribution is considered in present case to ease the analyses of results. To this aim, the constant pitch of the reference E779A geometry ($p/D = 1.12$) was replaced by a pitch distribution handled by a four control points B-Spline curve which range of variations, at fixed radial locations, are summarized in Table 1. This parametrization realizes the 4-dimensions design space used in the optimization process.

**Table 1**. Design parameters and relative ranges of variation.

| | control point 1 | control point 2 | control point 3 | control point 4 |
|---|---|---|---|---|
| $r/R$ | 0.2 | 0.6 | 0.9 | 1 |
| $p/D$ | [0.8 - 1.3] | [0.8 - 1.3] | [0.8 - 1.3] | [0.8 - 1.3] |

# 3 MULTIFIDELITY OPTIMIZATION OF THE E779A PROPELLER

## 3.1 Co-Kriging surrogate models for the KPI of E779A

The co-Kriging models for the KPI of propeller E779A were obtained as a combination of low-fidelity BEM calculations and high-fidelity RANS analyses. To analyse the goodness of the models, in principle, any combination of low- and high- fidelity samplings of the design space should be considered and validated by means of appropriate statistics on a subset of $M$ data for which computed results at both fidelity levels are available. Classical error measures are the percentage error $err\%$, defined in

Eq. 1, its mean $\overline{err\%}$, its standard deviation $\sigma(err\%)$ and the $R^2$ coefficient of determination of Eq. 2 which, all together, provide a picture of the surrogate model approximations. Index $i$ denotes the $i$-sample of the validation plan, the $\widehat{}$ refers to surrogate predictions and the $-$ denotes the average over the set of the samples for the validation.

$$err\%_i = \left| \frac{KPI_i - \widehat{KPI}_i}{KPI_i} \right| \cdot 100, \quad i = 1, \ldots, M \tag{1}$$

$$R^2 = 1 - \frac{\sum_{i=1}^{M} \left(KPI_i - \widehat{KPI}_i\right)^2}{\sum_{i=1}^{M} \left(KPI_i - \overline{KPI}\right)^2} \tag{2}$$

To simplify the analyses, co-Kriging models have been realized varying only the number of high-fidelity samples and then by always using the same set of low-fidelity data. To avoid an arbitrary choice, the Kriging models of the low-fidelity information at different sampling densities have been considered and compared with the aim of selecting the minimum set of data that realizes the convergence of the approximations. Samplings of the design space considered 40 to 640 configurations selected in the range of variations of the free parameters of Table 1 using the Sobol algorithm. A six-level full-factorial experiment, for a total of $M = 1296$ sampling points which were additionally evaluated using the BEM, was used instead for gathering the metrics of the models.

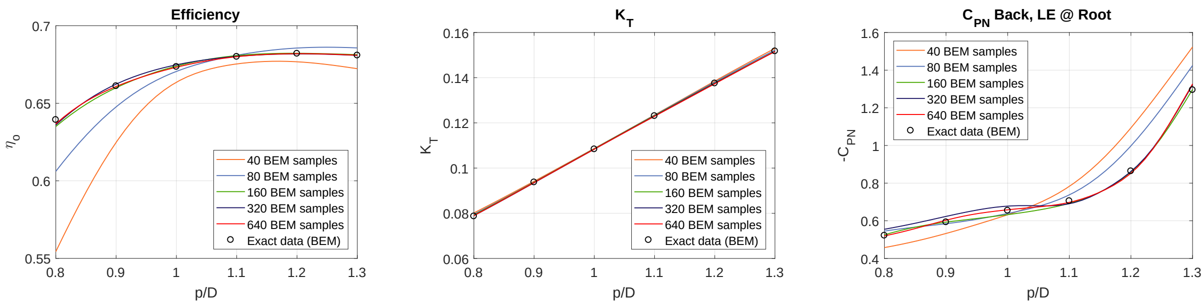


**Figure 2**. Convergence of surrogate approximation to "exact" (true BEM calculations) data for propeller efficiency, thrust and pressure coefficient (back side, leading edge at root). Data obtained for $p/D_1 = 0.8$, $p/D_2 = 1.133$ and $p/D_4 = 0.966$.

**Table 2**. Average error $\overline{err\%}$ of Kriging metamodels (BEM) for a selection of KPI.

| MetaModel | $\eta_o$ | $K_T$ | $C_{PN}$ Back, LE, Tip | $C_{PN}$ Back, LE, Root | $C_{PN}$ Face, LE, Root |
|---|---|---|---|---|---|
| B-40 | 1.72 | 0.84 | 14.57 | 9.64 | 5.88 |
| B-80 | 0.92 | 0.51 | 7.28 | 5.22 | 4.22 |
| B-160 | 0.49 | 0.35 | 5.82 | 3.66 | 2.68 |
| B-320 | 0.36 | 0.27 | 3.77 | 2.90 | 2.05 |
| B-640 | 0.13 | 0.21 | 2.27 | 1.89 | 1.28 |

**Table 3**. Coefficient of determination $R^2$ of Kriging metamodels (BEM) for a selection of KPI

| MetaModel | $\eta_o$ | $K_T$ | $C_{PN}$ Back, LE, Tip | $C_{PN}$ Back, LE, Root | $C_{PN}$ Face, LE, Root |
|---|---|---|---|---|---|
| B-40 | 0.609 | 0.998 | 0.983 | 0.962 | 0.990 |
| B-80 | 0.863 | 0.999 | 0.996 | 0.989 | 0.993 |
| B-160 | 0.955 | 1.000 | 0.997 | 0.993 | 0.998 |
| B-320 | 0.961 | 1.000 | 0.999 | 0.995 | 0.999 |
| B-640 | 0.994 | 1.000 | 1.000 | 0.997 | 0.999 |

The convergence trend, that is expressed, among the others, using the average error and the coefficient of determination of the metamodels for a selections of KPIs (Tables 2 and 3), is evident also by comparing the approximated propeller performances predicted by the response surfaces and shown in Figure 2. Decent approximations of experiments are possible already using 160 samples. Nevertheless,

the negligible computational cost of BEM calculations suggested the precautionary use of 320 points to limit any influence of these low-fidelity approximations on the co-Kriging models.
In the light of these results, six co-Kriging metamodels were trained using this constant set of 320 low-fidelity (B-, for BEM) points and a variable set of high-fidelity (R-, for RANS) data, from 4 to 40, selected in the design space again using Sobol (B-320/R-4, B-320/R-8, B-320/R-12, B-320/R-16, B-320/R-20, B-320/R-40). Some results, compared to single-fidelity Kriging response surfaces trained with the 320 low-fidelity BEM points or using only the same high-fidelity RANS data employed in the co-Kriging models, are shown in Figures 3 and 4. Their predictive capabilities are validated (and their statistics computed) with respect to a dedicated 4-levels full-factorial sampling of the design space (256 configurations) entirely solved using RANS analyses and assumed as the "exact" data to be matched by the surrogate models.

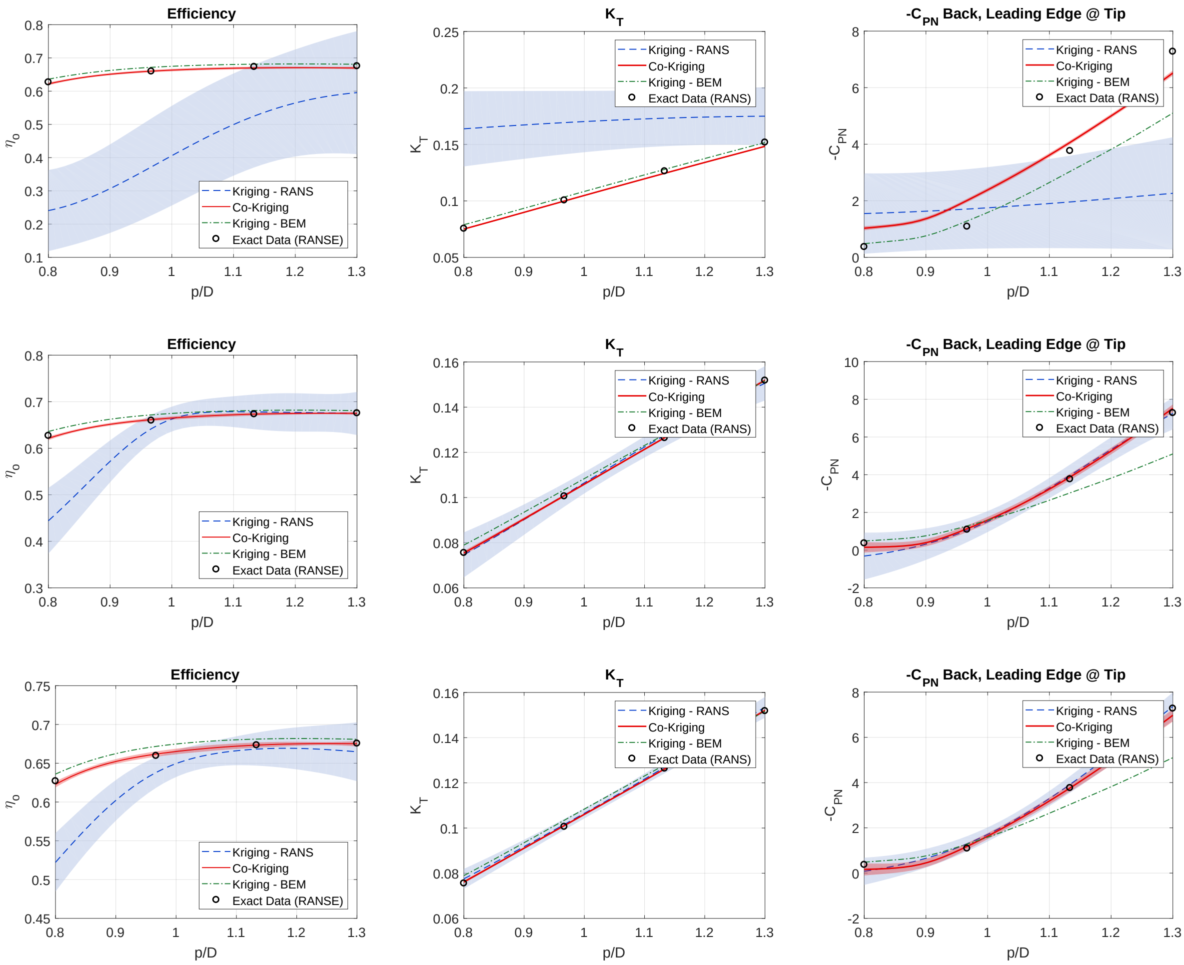


**Figure 3**. Convergence of co-Kriging metamodels to "exact" data (RANS) for propeller efficiency, thrust and pressure coefficient (back side, leading edge at tip). From top to bottom: B-320/R-4, B-320/R-16, B-320/R-40. Data obtained for $p/D_1 = 0.8$, $p/D_2 = 1.133$ and $p/D_4 = 0.966$.

**Table 4**. Average error $\overline{err\%}$ of co-Kriging metamodels for a selection of KPI. In parentheses the results of Kriging models trained using only the correspondent high-fidelity RANS samples.

| MetaModel | $\eta_o$ | $K_T$ | $C_{PN}$ Back, LE, Tip | $C_{PN}$ Back, LE, Root | $C_{PN}$ Face, LE, Tip |
|---|---|---|---|---|---|
| B-320/R-4 | 0.44 (11.3) | 1.50 (26.7) | 38 (128) | 63 (107) | 210 (2160) |
| B-320/R-8 | 0.19 (6.8) | 0.95 (2.0) | 27 (65) | 35 (50) | 195 (516) |
| B-320/R-12 | 0.17 (6.9) | 0.38 (1.5) | 29 (35) | 28 (29) | 167 (456) |
| B-320/R-16 | 0.11 (4.0) | 0.28 (1.4) | 19 (22) | 19 (27) | 226 (273) |
| B-320/R-20 | 0.10 (3.8) | 0.32 (1.0) | 19 (18) | 18 (28) | 132 (152) |
| B-320/R-40 | 0.06 (1.2) | 0.21 (0.5) | 12 (13) | 10 (17) | 133 (97) |

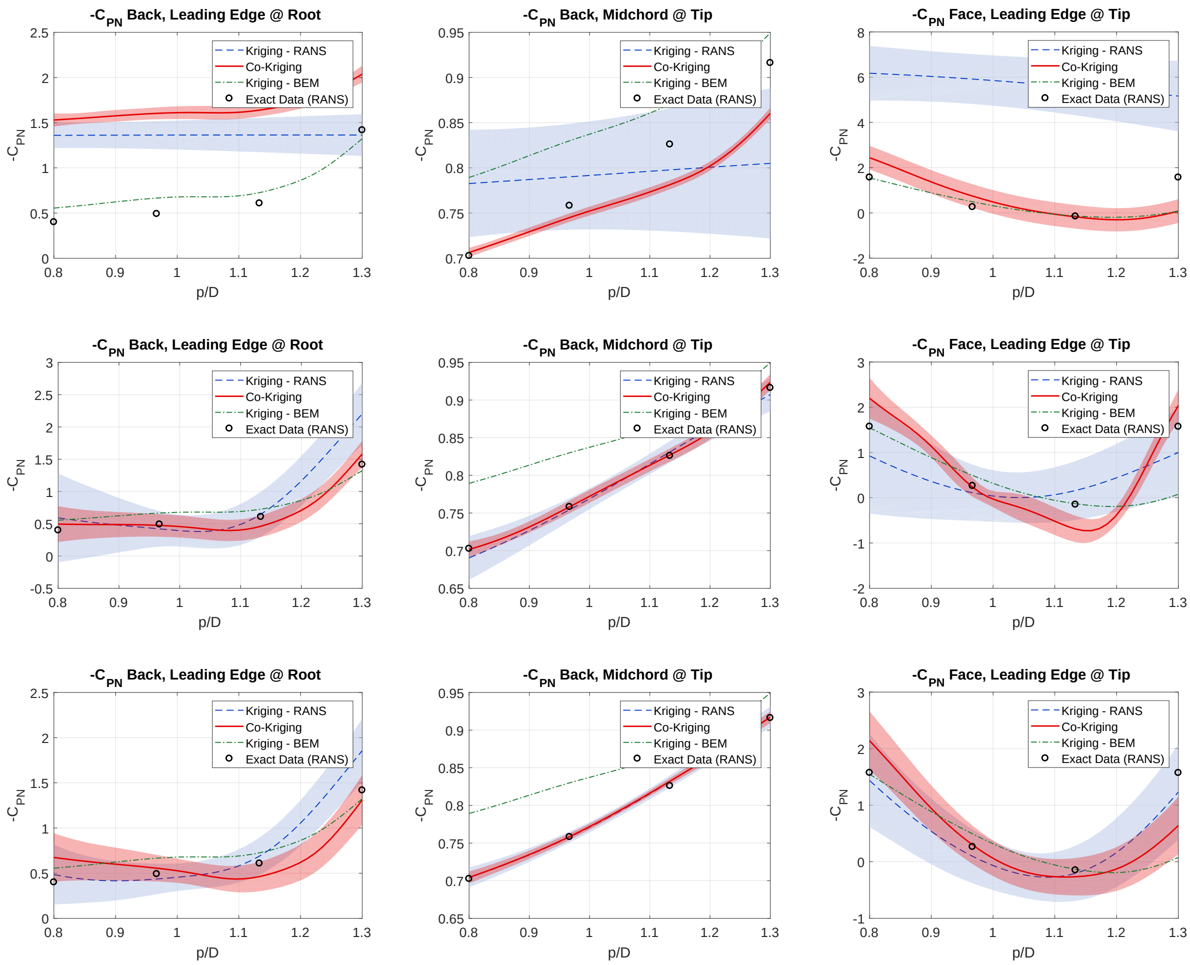


**Figure 4**. Convergence of co-Kriging metamodels to "exact" data (RANS) for pressure coefficient (back side, leading edge at root, midchord at tip and face side, leading edge at tip). From top to bottom: B-320/R-4, B-320/R-16, B-320/R-40. Data obtained for $p/D_1 = 0.8$, $p/D_2 = 1.133$ and $p/D_4 = 0.966$.

**Table 5**. Coefficient of determination $R^2$ of co-Kriging metamodels for a selection of KPI. In parentheses the results of Kriging models trained using only the correspondent high-fidelity RANS samples.

| MetaModel | $\eta_o$ | $K_T$ | $C_{PN}$ Back, LE, Tip | $C_{PN}$ Back, LE, Root | $C_{PN}$ Face, LE, Tip |
|---|---|---|---|---|---|
| B-320/R-4 | 0.969 (-30) | 0.995 (-0.086) | 0.935 (-0.003) | 0.472 (-0.392) | 0.690 (-2.021) |
| B-320/R-8 | 0.994 (-19) | 0.998 (0.993) | 0.947 (0.817) | 0.869 (0.192) | 0.719 (0.149) |
| B-320/R-12 | 0.995 (-11) | 0.999 (0.996) | 0.972 (0.967) | 0.896 (0.724) | 0.796 (0.383) |
| B-320/R-16 | 0.997 (-3) | 1.000 (0.996) | 0.981 (0.986) | 0.954 (0.871) | 0.777 (0.757) |
| B-320/R-20 | 0.998 (-4) | 1.000 (0.998) | 0.985 (0.989) | 0.959 (0.865) | 0.882 (0.760) |
| B-320/R-40 | 0.999 (0.3) | 1.000 (1.000) | 0.991 (0.994) | 0.991 (0.954) | 0.884 (0.917) |

Sustained by the metrics of the models, collected in Tables 4 and 5, the advantages of multi-fidelity approaches are clear for most of the KPI under investigation. Trends obtained by the low-fidelity data substantially help the predictive performances: the uncertainty levels associated to co-Kriging models are a fraction of those associated to single-fidelity surrogates trained using the same high-fidelity samples only and the average error is usually well below that from single-fidelity response surfaces. This is particularly true for B-320/R-4 and B-320/R-8 that enhance the predictive accuracy of the single-fidelity models at a negligible computational cost.

Increasing the number of high-fidelity points not always improves monotonically the performances of the surrogate models. While for quantities like the propeller efficiency, the thrust or the pressure on the back side at the tip of the leading edge there is no doubt about the opportunity of a multi-fidelity approach, for quantities like the pressure coefficient at the leading edge, on the tip of the face side, the usefulness of a co-Kriging metamodel has to be discussed. Few high-fidelity samples do not improve (or marginally improve) the performances of the two-fidelity level. The inclusion of some additional points (B-320/R-16, B-320/R-20) even makes single fidelity Kriging trained on this set of data more accurate than the co-Kriging. Moreover, the uncertainty associated to the predictions using the two-fidelity models is badly correlated to the actual error, preventing the possibility of successful adaptive samplings of the design space using this criterion. Reasons of this behaviour lie in the degree of correlation between the low- and the high-fidelity data, as discussed thoroughly by Forrester (Forrester et al., 2008, 2007) using analytical functions and in (Raven and Sholcz, 2019) for a similar CFD-based optimization case using multi-fidelity Kriging metamodels. A large degree of correspondence (i.e. $R^2 > 0.9$ as proposed byToal (2015)) between the data at different fidelity levels is required such that the trends provided by low-fidelity models can positively contribute to the accuracy of the response surface. A proof is given, for the KPIs discussed above, in Figure 5 where the performances of the single fidelity Kriging model using 40 RANS samples, when the correlation between BEM and RANS is poor, is better than that of the corresponding co-Kriging that uses also BEM data.

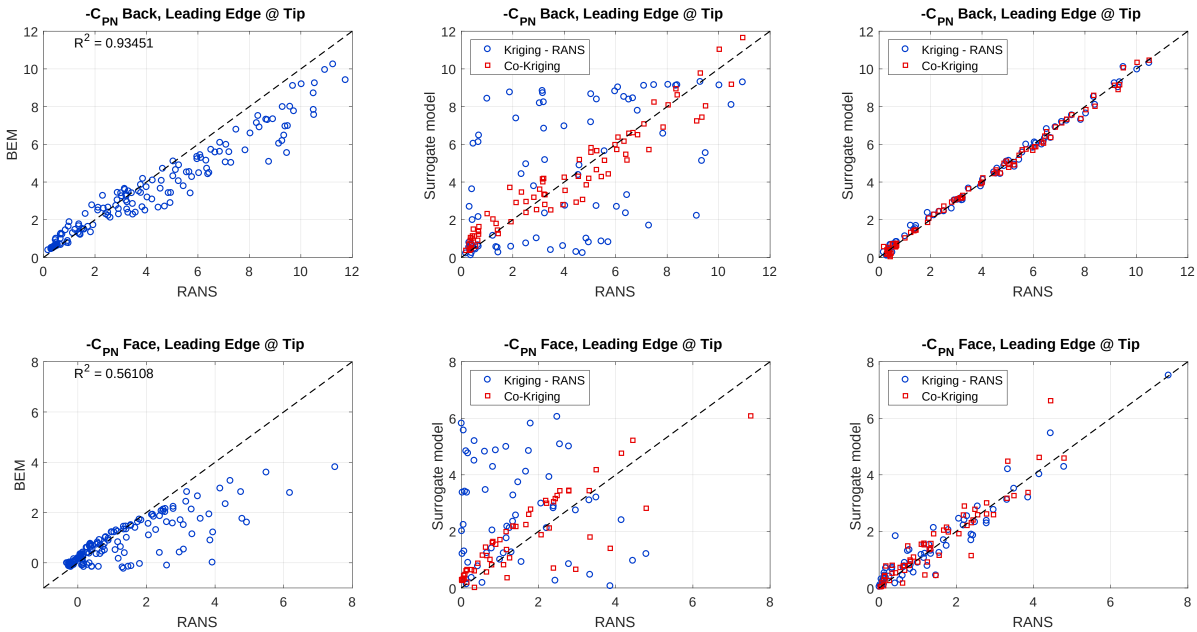


**Figure 5**. Correlations between low- (BEM) and high- (RANS) fidelity data (left) and “exact” and Kriging/co-Kriging approximations for two different models (B-320/R-4, middle, and B-320/R-40, right).

### 3.2 Co-Kriging based SBDO of E779A

The optimization problem, which has been considered in current work to demonstrate the benefits of a SBDO process using multi fidelity levels surrogate models, consists in the design of a new pitch distribution for the E779A propeller in order to:

$$\begin{aligned} \text{maximize} \quad & \eta_o(\mathbf{x}) \\ \text{minimize} \quad & -C_{PNi}(\mathbf{x}), i = 1..8 \\ \text{subject to} \quad & K_T(\mathbf{x}) = K_{Treference} \pm \epsilon \end{aligned} \tag{3}$$

where $\mathbf{x}$ is the design variable vector (i.e. the four $p/D$ values of the control points), $K_T$ and $\eta_o$ the delivered thrust and efficiency of the propeller and $-C_{PNi}$ the pressure coefficient collected in correspondence of the eight $i$ patches representative of the critical regions of the propeller for what concern the risk of cavitation. A tolerance ($\epsilon = 1\%$ of $K_{Treference}$) on the thrust constraint is applied to speed up the convergence process. The reference value for the thrust is that from BEM calculations of the reference propeller when the SBDO is applied using BEM outputs (i.e. direct analyses or

surrogates trained only with BEM data) or that from the preliminary RANS analysis of the original geometry when the SBDO makes use of response functions trained with RANS data.
The design was repeated six times (Design 1 to 6 in Figure 7) using, sequentially, the all the metamodels previously trained. The selection of the optimal geometries used a simplified criterion: regardless the position (tip or root), the selected geometry is the one that realizes the minimum risk of cavitation at the leading edge of the suction side. This is a single-objective criterion applied to a multi-objectives optimization but the aim, also in this applicative step of the procedure, is to compare the results of similarly selected geometries to assess the feasibility and robustness of the method and verify once again the convergence and the benefits of the two-fidelity levels approaches.
The performances of these propellers (direct RANS analyses and response surface outputs) are shown in Figure 7. Compared to the performances of the reference geometry, the optimization processes using surrogates always identified new propeller blades that deliver the same thrust, as prescribed in the SBDO, and reduce the cavitation inception at the leading edge of the suction side to a cavitation index of about 4 versus the value higher than 7 computed for the reference geometry (Figure 1). Efficiency is slightly reduced (of about 1%) and other quantities (inception index at midchord, for instance) are almost unchanged. This is a result of the selection criterion of optimal geometries which favours the minimization of leading edge phenomena rather than the balance of conflicting objectives. The correspondence between metamodels and direct RANS analyses is very good, in particularly for the quantities, like the propeller efficiency and thrust, that demonstrated lower uncertainties and very high levels of correlation also when using a very reduced number of high-fidelity samples to train the models.
A positive convergence of results when increasing the number of high-fidelity samples is observed as well: as the complexity of the surrogate models increases (design 1 to design 6), the estimated performances of the resulting optimized geometry using more accurate response surfaces are closer to those from direct RANS analyses. A better insight into this is given, moreover, in Figure 8 where the focus is on only one optimal geometry. The optimized propeller from design 1 (using the B-320/R-4 model) has been analysed using all the co-Kriging models trained with increasing number of samples. The predictions of the single-fidelity Kriging approximations based on the same RANS data (4 to 40 points) are shown as well, together with the KPI of this geometry calculated directly with BEM and RANS.
The comparison is explicative, once again, of the overall faster convergence trend granted by the inclusions of the low-fidelity data into the surrogate models and explain the different metrics (error and variance) of the models. As already discussed for this very simplified test case, a relatively small number of high-fidelity points is sufficient to train a single-fidelity Kriging model capable of predicting reasonably well some of the KPI of the problem. Thrust, or the pressure on the back side, can be reliably calculated also using a simple Kriging and a number of sampling point between 12 and 16 of this simple design space is sufficient for this. The uncertainty associated to efficiency and face side pressure distribution, for instance, requires instead the increasing of the samples of a single-fidelity Kriging model, even if trained using high-fidelity data, to stabilize the convergence to the exact values calculated using RANS. Co-Kriging, by leveraging the trends from low-fidelity data, for most of the KPI of the design ensures significantly better results (closer to exact RANS) thanks to an even lower number of high-fidelity samples since already 4 points definitely improve the predictive accuracy (and then the usability) of these surrogates. The same inconsistencies observed in the general trends of the models (i.e. estimated and calculated pressure distribution on the face side) can be observed also for the optimized propellers. The functioning point selected, that by itself mitigates the risks on the pressure side, makes these differences almost irrelevant for the scope of the design.

## 4 CONCLUSIONS

The feasibility of a Simulation Based Design Optimization approach using two-fidelity levels surrogate models based on co-Kriging response surfaces has been shown in the case of the design of a marine propeller. This approach blended low-fidelity data from a Boundary Element Method with high-fidelity

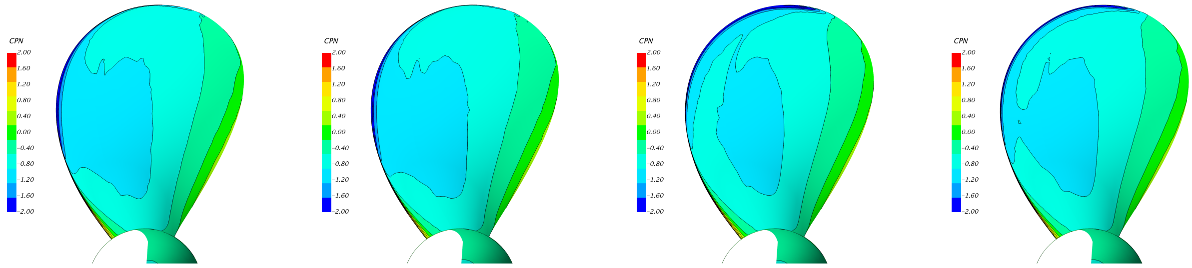

(a) Design 1, B-320/R-4 (b) Design 2, B-320/R-8 (c) Design 3, B-320/R-12 (d) Design 6, B-320/R-40

**Figure 6**. Pressure coefficient distributions (RANS analysis, back side) on some optimized propellers.

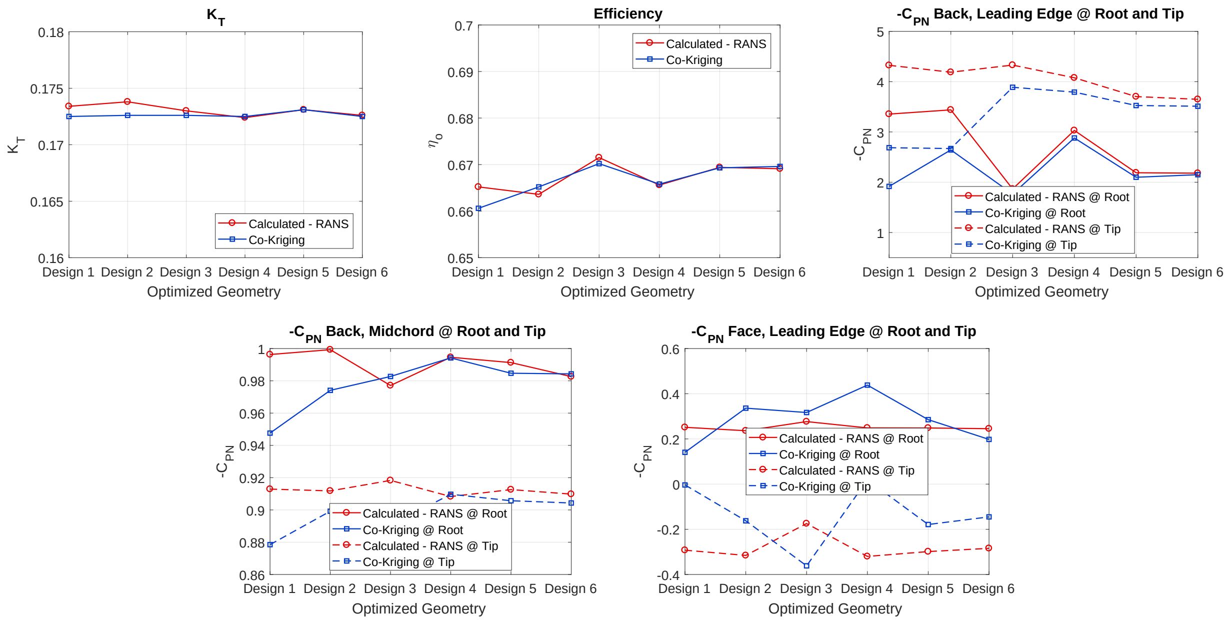


**Figure 7**. KPI of the selected propellers. Results refer to direct RANS calculations and outputs of the co-Kriging metamodels that were used for that particular design, i.e. KPI of Design 4 (optimization using B-320/R-16) are obtained using the same B-320/R-16 metamodels.

information from RANS analyses to improve the prediction capabilities of the response surfaces that substitute the expensive CFD analyses in the optimization process. A good agreement with calculated RANS data has been observed in the case of the design KPI estimated by using these approximated models. This agreement is higher, for instance, than that granted by single-fidelity surrogate models trained on the few available high-fidelity samples and, obviously, than results obtainable by only low-fidelity BEM calculations. The verification using direct RANS analyses of the optimized propellers identified by the surrogate models confirms these trends. It demonstrates how complex and expensive explorations of the design space, aimed at optimization or identification of design guidelines, can take advantage of these techniques, which at a very reduced computational cost (in this case, from 4 to 8 high-fidelity calculations) significantly improve the predictive accuracy of metamodels that sometimes are the only possible approaches to deal with a design problem using the paradigm of optimization. On the other hand, the systematic analysis of several KPI shown possible limitations of these multi-fidelity surrogate models, which require a large degree of correspondence between the fidelity levels to positively contribute to the accuracy of the response surface. In current analyses the estimation of the pressure on the face side of the propeller encountered these issues, sometimes related to imperfections in the discretization using BEM and RANS. Improving these correspondence (by different meshing approaches) and including adaptive samplings of the design space could further improve the predictive accuracy at even lower computational costs.

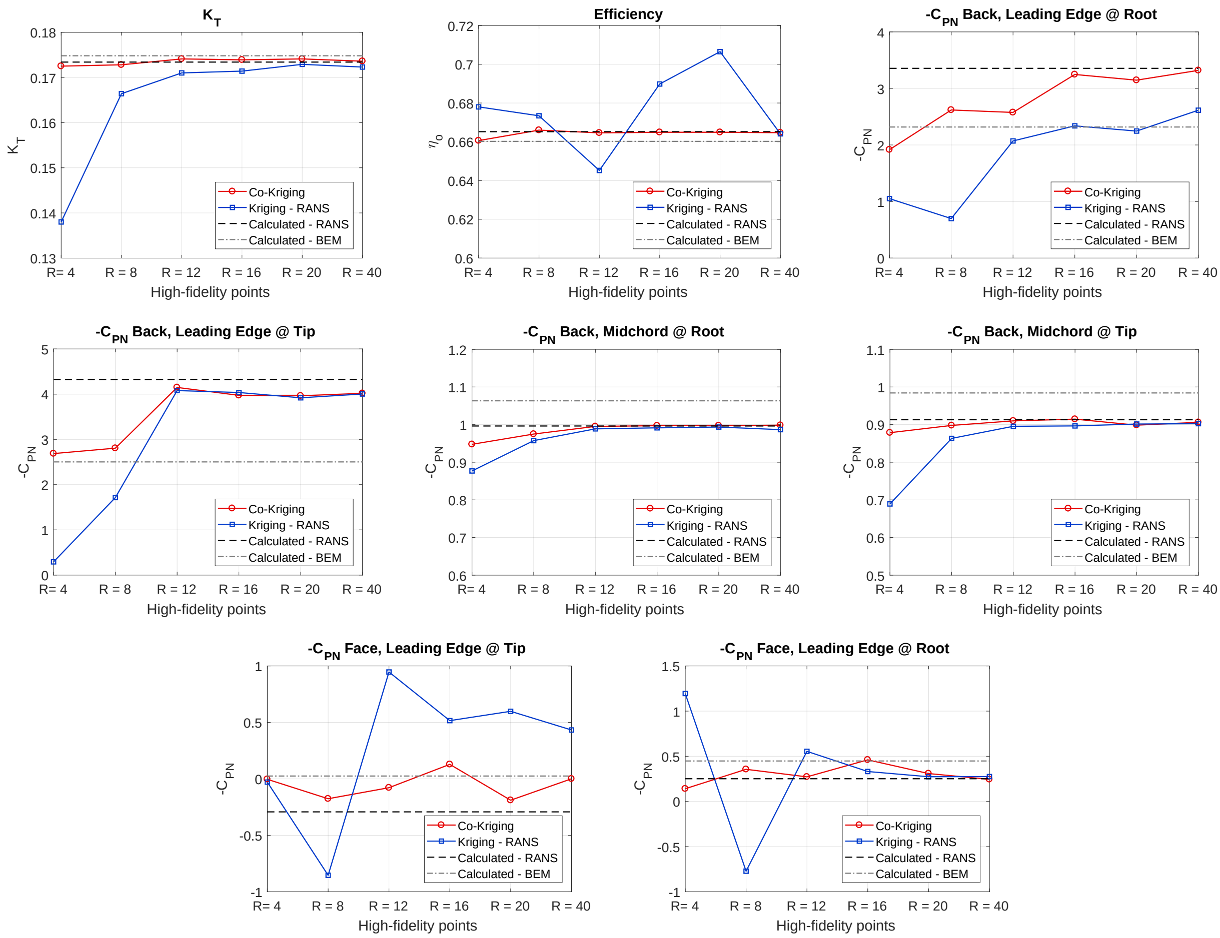


**Figure 8**. Convergence of co-Kriging results to RANS calculations with the number of high-fidelity samples. Comparison with Kriging response surfaces trained using the same high-fidelity samples. Design case 1, B-320/R-4.

## References

Coppedè, A., Gaggero, S., Vernengo, G., and Villa, D. (2019). Hydrodynamic Shape Optimization by High Fidelity CFD Solver and Gaussian Process Based Response Surface Method. *Applied Ocean Research*, 90:101841.

Coppedé, A., Vernengo, G., and Villa, D. (2018). A Combined Approach Based on Subdivision Surface and Free Form Deformation for Smart Ship Hull Form Design and Variation. *Ships and Offshore Structures*, 13(7):769–778.

Couckuyt, I., Dhaene, T., and Demeester, P. (2014). ooDACE toolbox: a Flexible Object-Oriented Kriging Implementation. *Journal of Machine Learning Research*, 15:3183–3186.

de Baar, J., Roberts, S., Dwight, R., and Mallol, B. (2015). Uncertainty Quantification for a Sailing Yacht Hull, using Multi-Fidelity Kriging. *Computers & Fluids*, 123:185–201.

Forrester, A., Sobester, A., and Keane, A. (2008). *Engineering Design via Surrogate Modelling: a Practical Guide*. John Wiley & Sons.

Forrester, A. I. J., Sóbester, A., and Keane, A. J. (2007). Multi-Fidelity Optimization via Surrogate Modelling. *Proceedings of the royal society a: mathematical, physical and engineering sciences*, 463(2088):3251–3269.

Gaggero, S. (2020). Numerical Design of a RIM-Driven Thruster using a RANS-Based Optimization Approach. *Applied Ocean Research*, 94:101941.

Gaggero, S., Coppedé, A., Villa, D., Vernengo, G., and Bonfiglio, L. (2019). A D]ata-Driven Probabilistic Learning Approach for the Prediction of Controllable Pitch Propellers Performance. In *MARINE VIII: proceedings of the VIII International Conference on Computational Methods in Marine Engineering*, pages 544–555. CIMNE.

Gaggero, S., Gonzalez-Adalid, J., and Sobrino, M. P. (2016). Design and Analysis of a New Generation of CLT Propellers. *Applied Ocean Research*, 59:424–450.

Gaggero, S., Villa, D., and Viviani, M. (2014). An Investigation on the Discrepancies between RANSE and BEM Approaches for the Prediction of Marine Propeller Unsteady Performances in Strongly non-homogeneous Wakes. In *International Conference on Offshore Mechanics and Arctic Engineering*.

Morino, L. and Kuo, C. (1974). Subsonic Potential Aerodynamics for Complex Configurations: a General Theory. *AIAA journal*, 12(2):191–197.

Raven, H. C. and Sholcz, T. P. (2019). An Assessment of Multifidelity Procedures for Ship Hull Form Optimisation. In *MARINE VIII: proceedings of the VIII International Conference on Computational Methods in Marine Engineering*, pages 189–200. CIMNE.

Serani, A., Pellegrini, R., Wackers, J., Jeanson, C.-E., Queutey, P., Visonneau, M., and Diez, M. (2019). Adaptive Multi-Fidelity Sampling for CFD-Based Optimisation via Radial Basis Function Metamodels. *International Journal of Computational Fluid Dynamics*, 33(6-7):237–255.

Toal, D. J. J. (2015). Some Considerations Regarding the Use of Multi-Fidelity Kriging in the Construction of Surrogate Models. *Structural and Multidisciplinary Optimization*, 51(6):1223–1245.

Wang, G. G. and Shan, S. (2007). Review of Metamodeling Techniques in Support of Engineering Design Optimization. *Journal of Mechanical Design*, 129:370–380.